Acta Biomaterialia xxx (2015) xxx–xxx

Contents lists available at ScienceDirect

Acta Biomaterialia

journal homepage: www.elsevier.com/locate/actabiomat

Full length article

Platelet lysate-based pro-angiogenic nanocoatings

Sara M. Oliveira, Rogério P. Pirraco, Alexandra P. Marques, Vítor E. Santo, Manuela E. Gomes, Rui L. Reis, João F. Mano *

3B's Research Group – Biomaterials, Biodegradable and Biomimetics, Avepark – Parque de Ciência e Tecnologia, Zona Industrial da Gandra, 4805-017 Barco – Guimarães, Portugal
ICVS/3B's – PT Government Associate Laboratory, Braga/Guimarães 4805-017, Portugal

ARTICLE INFO

Article history:
Received 2 September 2015
Received in revised form 10 December 2015
Accepted 15 December 2015
Available online xxxx

Keywords:
Layer-by-layer assembling
Instructive surfaces
Platelet lysate
Growth factors
Angiogenesis
Endothelial cells

ABSTRACT

Human platelet lysate (PL) is a cost-effective and human source of autologous multiple and potent pro-angiogenic factors, such as vascular endothelial growth factor A (VEGF A), fibroblast growth factor b (FGF b) and angiopoietin-1. Nanocoatings previously characterized were prepared by layer-by-layer assembling incorporating PL with marine-origin polysaccharides and were shown to activate human umbilical vein endothelial cells (HUVECs). Within 20 h of incubation, the more sulfated coatings induced the HUVECS to the form tube-like structures accompanied by an increased expression of angiogenic-associated genes, such as angiopoietin-1 and VEGF A. This may be a cost-effective approach to modify 2D/3D constructs to instruct angiogenic cells towards the formation of neo-vascularization, driven by multiple and synergistic stimulations from the PL combined with sulfated polysaccharides.

Statement of Significance

The presence, or fast induction, of a stable and mature vasculature inside 3D constructs is crucial for new tissue formation and its viability. This has been one of the major tissue engineering challenges, limiting the dimensions of efficient tissue constructs. Many approaches based on cells, growth factors, 3D bioprinting and channel incorporation have been proposed. Herein, we explored a versatile technique, layer-by-layer assembling in combination with platelet lysate (PL), that is a cost-effective source of many potent pro-angiogenic proteins and growth factors. Results suggest that the combination of PL with sulfated polyelectrolytes might be used to introduce interfaces onto 2D/3D constructs with potential to induce the formation of cell-based tubular structures.

1. Introduction

The development of tissue engineering constructs containing a functional and mature pre-vasculature is still a major challenge [1–3]. In the absence of such a network, the viability and regeneration potential of thick constructs will be compromised due to the limitation of nutrients and cell debris diffusion. In order to overcome this issue, researchers have been recurring either to material-based and cell-based approaches aiming to create an adequate vasculature inside engineered constructs. Material-based approaches have been focusing on the development of cellular or acellular 3D organized vessel-like structures through microfabrication and customized cell seeding methodologies [4,5]. On the other hand, cell-based approaches have been centered the instruction and activation of the involved angiogenic cells (e.g., endothelial and pericytes) to lead their cellular assembling into stable cellular tubular networks (i.e., tubulogenesis). The specific instruction of endothelial cells (EC) towards the formation of stable tube-like structures (TLS) has been extensively investigated [6,7]. Natural or synthetic extracellular cues such as collagen, fibrin, growth factors (GFs) or similar epitopes, are known to activate specific integrins and tyrosine kinase receptors, efficiently promoting angiogenic cells activation and formation of TLS. However, most of those instructive cues/constructs are frequently obtained from animal-origin and costly sources, or need complicated procedures. The formation of neo-vessels involves a complex crosstalk between several cell types, platelets releasates, extracellular matrix and their secreted pro and anti-angiogenic factors. Vascular endothelial growth factor (VEGF) and fibroblast growth factor b (FGFb) are considered the most potent angiogenic GFs being frequently used to

* Corresponding author at: University of Minho, 3B's Research Group, Avepark – Parque de Ciência e Tecnologia, Zona Industrial da Gandra, 4805-017 Barco – Guimarães, Portugal.
E-mail address: jmano@dep.uminho.pt (J.F. Mano).

http://dx.doi.org/10.1016/j.actbio.2015.12.028
1742-7061/

prepare angiogenic biomaterials. The angiogenesis is initiated and regulated by several cells types, GFs and other bioactive proteins and environmental cues such as hypoxia [8]. The ECs are activated, proliferate, migrate and, in the final stage, their tubular structures are stabilized by pericytes, smooth vascular cells and synthetized ECM [8].

Recent works have been highlighting the importance of the provision of multiple GFs in order to achieve better networks regarding size features and stability [1,9–12]. This has been explored by the combination of multiple recombinant GFs or other cell types able to provide such bioactive moieties to the EC. Platelets, natural players in the healing process, are very attractive sources of multiple GFs, metalloproteinases and other potent regulators of angiogenesis [13].

The ability of platelets derivatives to stimulate ECs proliferation, migration and enhance *in vitro* and *in vivo* angiogenesis has been recently reported [9,14–20]. These features has been mainly attributed to platelet-rich-plasma (PRP). PRP has been mixed with biomaterials [9,18,19], adsorbed onto scaffolds [20], used as PRP-gel [17] or by itself [14–16]. Moreover, reports have shown that PRP, used as extract in GFs-reduced Matrigel, can promote the formation of tube-like structures (TLS) of ECs within less than 24 h, which reinforces its angiogenic potential [14–16]. However, Matrigel or other similar rich basement membranes are from animal sarcoma origin, thus are not considered a suitable option for human application [21].

Herein, we propose the reconstruction of angiogenic nanobasement membranes-like constructs by using platelet lysate (PL) – as a source of multiple angiogenic factors-, marine-origin polysaccharides – as stabilizers -, and layer-by-layer assembling (LbL) – for a controlled assembling – Fig. 1a. PL was obtained by lysing human platelet concentrates by freezing-thawing cycles – Fig. 1b.

LbL is a simple and versatile technique comprising the alternated deposition of polyelectrolytes (PEs) interacting by electrostatic, or other types of interactions, and can be performed under mild conditions [22–24]. In order to achieve an efficient EC activation mediated by GFs, their stability, conformation and density presented to the cells must be adequate. Moreover, the type of binding between the GF and their stabilizer will affect the intracellular signal transduction [25] – Fig. 1c. Under this context, several PEs were assembled with PL, and in order to preliminarily assess the pro-angiogenic potential of the nanocoatings, human umbilical vein ECs (HUVECs) adhesion, proliferation, morphology and gene expression were analyzed.

2. Materials and methods

2.1. Materials

Medium molecular weight chitosan (Chi), with a degree of deacetylation of 80% (Sigma Aldrich, MKBB0566), was purified by a re-precipitation method. Briefly, Chi powder was dissolved in 2% (v/v) acetic acid solution with 1% (w/v) concentration. The mixture was stirred overnight at room temperature. The impurities were removed by four filtration cycles. Then, Chi was precipitated by addition of 1 M NaOH while stirring. Final steps consisted on washing Chi with distilled water until reaching a neutral pH and on Chi dehydration rising with ethanol–water mixtures with increasing ethanol content (20–100% v/v). Chi was freeze-dried for 3 days and ground. κ- (Sigma–Aldrich, 22048), ι- (Fluka, 22045), λ-carrageenan (Car; Sigma–Aldrich, 22049), sodium heparin (Hep; Sigma–Aldrich, H3149), sodium alginate (Alg; Sigma Aldrich, 250 cP), and poly(ethyleneimine) solution (PEI; Sigma–Aldrich, P3143) were used as received.

2.2. Materials preparation

2.2.1. Preparation of platelet lysate

Platelet concentrates were obtained from different platelet collections performed at Instituto Português do Sangue (IPS, Porto, Portugal), under a previously established cooperation protocol. The components were obtained using the Trima Accel® Automated Blood Collection System. All the platelet products were biologically qualified according to the Portuguese legislation. The platelet count was performed at the IPS using the COULTER® LH 750 Hematology Analyzer and the sample volume adjusted to 1 million platelet μL^{-1}. The collected samples were subject to three repeated temperature cycles (frozen with liquid nitrogen at −196 °C and heated at 37 °C) and frozen at −20 °C until further use. The remaining platelets were eliminated by centrifugation at

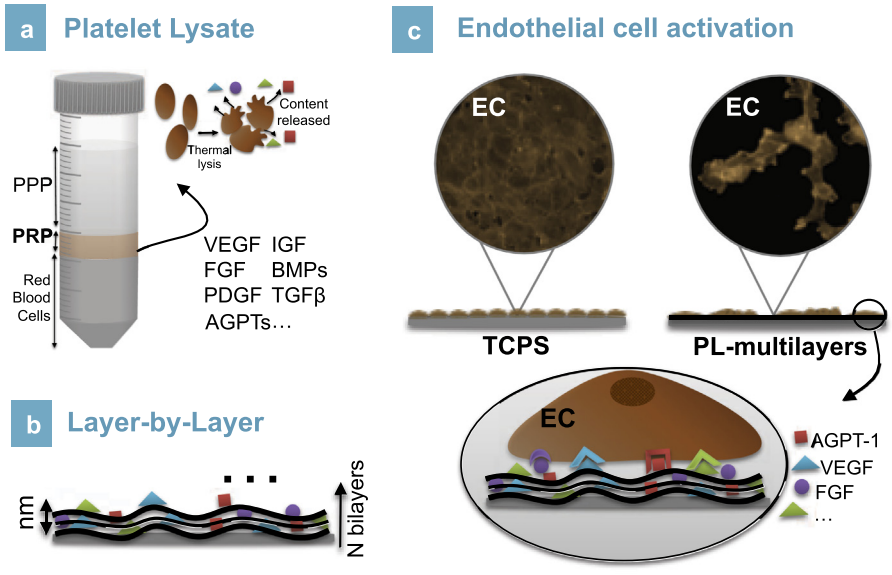

Fig. 1. Schematic representation of the approach followed. (a) PL preparation. (b) Layer-by-Layer assembling onto tissue culture polystyrene (TCPS) surfaces. (c) Culture of endothelial cells (ECs) during 20 h on the nanocoatings and expected interaction through VEGF, FGF, Angiopoietin-1 and other receptors.

Please cite this article in press as: S.M. Oliveira et al., Platelet lysate-based pro-angiogenic nanocoatings, Acta Biomater. (2015), http://dx.doi.org/10.1016/j.actbio.2015.12.028

1400*g* for 10 min. Aliquots of Platelet lysate (PL) were stored at −20 °C until final use. This procedure has not jeopardized growth factors bioactivity [26].

2.2.2. Polyelectrolytes solutions

κ-, ι-, λ-Car, Hep and Alg were prepared in 1 M Tris HCl 40 nM NaCl pH 7.4 at a concentration of 0.5 mg mL^{-1}. Chi was dissolved in sodium acetate buffer at a concentration of 0.5 mg mL^{-1}. PL was 10-fold diluted with Tris HCl buffer for the multilayers with Car, Hep and Alg, or with 1 M sodium acetate 40 mM NaCl pH 6 to be combined with Chi.

2.2.3. Coatings preparation in 48-well plates

In order to prepare coatings with 6 bilayers of the pairs Alg/PL, Chi/PL, κCar/PL, ιCar/PL, λCar/PL and Hep/PL, all 48-well plates were modified with 0.5 mL of 0.5% (w/v) PEI solution to confer a positive surface charge. Then, the solution was removed and the wells were extensively rinsed with distilled water in order to remove the unbound PEI. LbL assembling was started by the adsorption of the negative PE. In the case of Chi, an Alg layer was first adsorbed which was followed by Chi. The adsorption times and volumes used were: 4 min and 0.5 mL for the polysaccharides solutions; 0.5 mL and 10 min for the PL solution; intermediate rising steps x2 for 30 s using the respective buffers. The sequence was repeated 1, 3 or 6 times. The well plates were let to air-dry overnight and then sterilized using a UV light for 40 min.

2.3. Cell behavior assessment

2.3.1. HUVECs isolation

Human umbilical cords obtained after caesarean sections from healthy donors were provided by Hospital de S. Marcos, Braga, Portugal. They were delivered in transport buffer, containing 0.14 M NaCl, 0.004 MKCl and 0.011 M glucose in 0.001 M phosphate buffer at pH 7.4. Human umbilical cord vein endothelial cells (ECs) (HUVECS) were isolated as described in literature by Jaffe and others [1].

Biological samples were provided under a protocol approved by the Hospitals Ethical Committees and the 3B's Research Group. Cells were expanded using M199 supplemented with 50 μg/mL endothelial cell growth supplement (ECGS, BDBiosciences), 50 μg/mL of heparin, 3.4 μl/mL Gibco® GlutaMAX™ (Life Technologies) and 20% fetal bovine serum (FBS). Cells were cultured at 37 °C, 5%CO_2, 99% humidity and medium was exchanged every 2–3 days. HUVECs from two different donors and between passage 4 and 7 were used in the experiments.

2.3.2. Cell culture

To proceed with the cell seeding, expanded cells were harvested by trypsinization and filtered with a 100 μm cell strainer to remove possible cell aggregates. Different cell densities were prepared: 20,000 cells/mL with 0% FBS, 20,000 cells/mL with 10% FBS, 20,000 cells/mL with 20% FBS for cell adhesion and proliferation quantification; 100,000 cells/mL, 200,000 cell/mL, 300,000 cells/mL with 10% FBS for cell morphology studies. A volume of 500 μL of cell suspension was dispensed into each well. Well-plates were incubated for 20 h. After that, medium was replaced with fresh one with 10% FBS, ECGS and sodium heparin for proliferation quantification. Medium without ECGS and sodium heparin was used as control.

For FGF/VEGF blockage test, M199 medium was supplemented with 10% FBS and DMSO or FGF/VEGF Receptor Tyrosine Kinase Inhibitor (PD173074, Santa Cruz Biotechnology), dissolved in DMSO. According with the manufacturer, it is (N-[2-[[4-(Diethylamino)butyl]amino]-6-(3,5-dimethoxyphenyl)pyrido[2,3-d]pyrimidin-7-yl]-N′-(1,1-dimethylethyl)urea) a potent inhibitor of many VEGF and FGF receptors.

HUVECs (50,000 cells/500 uL) were seeded onto 1 cm^2-coated well plates and cultured for 20 h in medium supplemented with 150 nM (0.0075% in DMSO) or 200 nM (0.01% in DMSO) of inhibitor and only DMSO (0.0075% and 0.01%).

2.3.3. Cytoskeleton staining

After 20 h or 4 h in culture, samples were gently rinsed twice with sterile PBS and then fixed with formalin 10% (v/v) during 20 min. Cells were permeabilized with 0.5 mL of Triton 0.2% (v/v) in PBS during 2 min and then rinsed with PBS. Samples were incubated in the dark with 100 μL of (1:100) Phalloidin-TRITC (Sigma–Aldrich) solution for 30 min and then washed with PBS. For cell nuclei staining, well plates were incubated in the dark for 5 min with 100 μL 4,6-diamino-2-phenyindole dilactate (DAPI, Sigma–Aldrich) diluted 1:1000 in PBS. Samples were observed using an inverted Axio Observer Fluorescence Inverted Microscope (Zeiss, Germany) and random images recorded for analysis.

2.4. Image analysis

2.4.1. Angiogenesis analyzer

Angiogenesis Analyzer, a toolset of Image J software, allowed the analysis of cellular networks.

The total length of the tube-like structures, number of nodes and of master nodes, number of meshes and of master meshes were quantified on cytoskeleton fluorescence images of HUVECs after 20 h of culture. A node was defined as pixels that have at least 3 neighbors, corresponding to a bifurcation. A junction was considered a node or fused nodes. The segments correspond to elements that were limited by two junctions/nodes while the branches were elements delimited by a junction and one extremity. The master segments were considered pieces of three, delimited by two junctions, but not exclusively implicated with one branch (master junctions). The master junctions linked at least 3 master segments. The meshes were defined as areas enclosed by the segments or master segments.

2.4.2. Cell profiler

Cell Profiler [43] allowed analysing the morphological changes of HUVECs when cultured for 20 h on coatings, in the presence or absence of inhibitors. was Eccentricity, form factor and major and minor axis length features available with Cell Profiler analysis were used. The values of eccentricity is defined as the ratio of the distance between the foci of the considered ellipse and its major axis length. The values vary between 0 and 1. Values equal to zero are actually circles while ellipses with eccentricity of 1 are lines. The form factor was calculate as 4π(Cell Area)/(Cell Perimeter)2, where 1 represent a perfect circular cell. The major and minor axis length (in pixels) correspond to the major and minor axis of the ellipse, respectively. The images used for Cell Profiler analyses were the same as for Angiogenesis Analyzer.

2.5. dsDNA quantification

In order to quantify cell attachment after 20 h and proliferation up to 4 days in culture, dsDNA was quantified using the Quant-iT™ PicoGreen® dsDNA assay kit (Molecular Probes/Invitrogen) following the manufacturer instructions. After the incubation periods, the well plates were gently rinsed once with sterile PBS. Then, 1 mL of ultra-pure sterile water added and kept at −80 °C until quantification. For the quantification, samples were defrosted at room temperature and the fluorescence was read in a microplate reader at an excitation wavelength of 485 nm and emission wavelength of 528 nm. A standard curve was created by varying

the concentration of standard dsDNA standard from 0 to 2 mg mL^{-1}. dsDNA values of the samples were read off from the standard graph. At least five specimens were measured per each sample.

2.6. Real time RT-PCR

The quantification of angiogenic gene expression (Table 1) of the HUVECS cultured on the coatings and on TPCS during 20 h, was performed using quantitative PCR by a two-step fluorogenic assay using the PerfeCta™ SYBR® Green System (Quanta Biosciences).

The total RNA was extracted using the TRI® Reagent (Sigma–Aldrich), following the manufacturer's instructions and then quantified using Nanodrop® ND-100 spectrophotometer (thermo Scientific). First-strand complementary DNA (cDNA) was synthetized using 1 μg RNA of each sample and the qScriptTM cDNA Synthesis Kit (Quanta Biosciences) for a 20 μL reaction. The obtained cDNA was used as a template for the amplification of the target genes using a MasterCycler EP Gradient detection System (Eppendorf) thermocycler and the PerfeCtaTM SYBR® Green System kit following the manufacturers' instructions. The Livak method, $2^{-\Delta\Delta Ct}$, was used to evaluate the relative expression of each target gene. ΔCt was calculated by the difference between the Ct values of the target gene and the β-actin or GAPDH endogenous housekeeping gene. ΔΔCt was obtained by subtracting the ΔCt of the calibrator sample (TCPS) to the ΔCt of the sample. The results are represented as $2^{-\Delta\Delta Ct}$ and as gene expression relative to TCPS.

2.7. Statistical analysis

The normality of the data was verified with Shapiro–Wilk test. All data was then statistically analyzed using non-parametric tests. The unpaired one-tailed *t*-test with Welch's correction for non-parametric data was used ($p \leqslant 0.05$).

3. Results and discussion

In the natural ECM, glycosaminoglycans presenting various molecular arrangements, as well as different sulfation degrees (SD), bind and stabilize GFs mainly by electrostatic interactions [27–29]. Heparin, or synthetic heparin-analogue ending sulfate groups, are widely used to stabilize and attract GFs [30–31]. Since they present high affinity and the interactions are mainly electrostatic, the conformation and bioactivity of the GFs is usually preserved. Natural resources, including those from marine-origin, offer a wide range of PEs with several molecular properties and SD that may affect the incorporation of GFs from PL onto the coatings [32–34]. Therefore, marine-origin polysaccharides were considered convenient and cost-effective sources of PEs to attract, stabilize, buildup and tune PL nanocoatings prepared by LbL assembling [35]. We hypothesize that such combination of PEs and PL could be an adequate strategy to deconstruct fundamental structural and functional aspects of the extra-cellular matrix towards the design of clinically relevant tissue engineering constructs able to stimulate angiogenesis [36]. PEs with different charge and functional groups were combined with PL, namely: alginate (Alg; −1) and chitosan (Chi; +1), as non-sulfated PEs; and κ-, ι-, and λ-carrageenan (κCar, ιCar, λCar; −1, −2, −3 respectively), as sulfated PEs; along with heparin (Hep; −3), as a control sulfated PE. In a previous work [26], the capability of these PEs to sequester fibroblast growth factor b (FGFb), vascular endothelial growth factor A (VEGF A) and platelet derived growth factor (PDGF) from PL during the assembling was analyzed. It has been observed that the content of those GFs in the nanocoatings (30–50 thick with 6 bilayers) was highly influenced by the nature of the PE. Briefly, the sulfated PEs and Hep were able to adsorbed higher levels of GFs; however, higher SD did not imply enhanced incorporation. Namely, PDGF adsorption was decreased with the increase of SD, while the highest contents of VEGF A reached were detected on Hep and ιCar. Interestingly, ιCar was able to adsorb a high amount of all the measured GFs. Consequently, higher SD represented nanocoatings with increased VEGF A/PDGF and FGFb/PDGF ratios suggesting them to be more adequate for the morphogenic activation of EC.

Table 1
Sequences and melting temperature of the angiogenic genes analyzed.

Gene	Primer sequence (Forward, Reverse 5′–3′)	Tm (°C)
β-actin	ACTGGAACGGTGAAGGTGAC AGAGAAGTGGGGTGGCTTTT	59.5
GAPDH	ACAGTCAGCCGCATC GACAAGCTTCCCGTTCTCAG	58.4
Integrin β3	ACCAGTAACCTGCGGATTGG TCCGTGACACACTCTGCTTC	59.4
Integrin αv	CCGATTCCAAACTGGGAGCA GGCCACTGAAGATGGAGCAT	59.4
Integrin α5	TGGCCTTCGGTTTACAGTCC GGAGAGCCGAAAGGAAACCA	59.4
VEGFA	GACAGATCACAGGTACAGGG AGAAGCAGGTGAGAGTAAGC	58.4
FGFb	GAGCAAATCTGCCCTGCTCA TCCCGCATACTCTGGAGACA	59.4
Angiopoietin-1	GAAGGGAACCGAGCCTATTC GGGCACATTTGCACATACAG	58.4

3.1. Endothelial cells adhesion

The HUVECs were seeded onto coatings of PL with 6 bilayers of Alg/PL, Chi/PL, κCar/PL, ιCar/PL, λCar/PL and Hep/PL, in the absence of both EC growth supplement (ECGS) and Hep, and with varied concentrations of fetal bovine serum (FBS, 0%, 10% and 20%) up to 20 h – Fig. 2a.

In absence of serum, the adhesion of HUVECs was limited and the number of cells in all the coatings and in the tissue culture polystyrene (TCPS) was similar – Fig. 2a. Comparing to TCPS, with 10% FBS, cell adhesion was not significantly affected by the presence of the multilayers with exception of Alg and Chi ($p < 0.05$) – Fig. 2b. Increasing the content of FBS to 20% has also not altered much the adhesion of HUVECS relatively to TCPS – Fig. 2c. Nonetheless, in presence of serum, HUVECS tended to adhere more on ιCar/PL_6 ($p < 0.05$). On the other hand, the Chi/PL and Alg/PL nanocoatings showed a tendency to impair cell adhesion ($p < 0.05$), independently on the concentration of FBS.

3.2. Endothelial cells morphology

The ability of those multilayers to activate ECs towards the formation of tube-like structures (TLS) was also assessed. HUVECs were seeded with a density of 100,000 cells/cm^2 in presence of 10% FBS and their morphology was observed after 20 h of incubation. Fig. 3 and Fig. S1 show the HUVECs morphology on all the assessed conditions. λ/PL_6 and Hep/PL_6 induced considerably higher cell cohesion, forming branching anastomosing tubes-like with multicentric junctions giving rise to a network of TLS – Fig. 4. No clear TLS were observed in Alg/PL_6, Chi/PL_6 nor ι/PL_6. Although Chi and Alg PEs significantly adsorb PL [26], the nature or stability of their pro-angiogenic cues were not enough to induce the cellular assembling. In the case of ι/PL, TLS structures were observed under other cell density conditions (53,000 cells/cm^2) – Fig. S2. The ECs highly adhered onto ι/PL_6, which is believed to consequently inhibit TLS formation. This might be caused by VE cadherin complexation with VEGF receptor, which inhibits its phosphorylation by VEGF and consequently the formation of TLS [37].

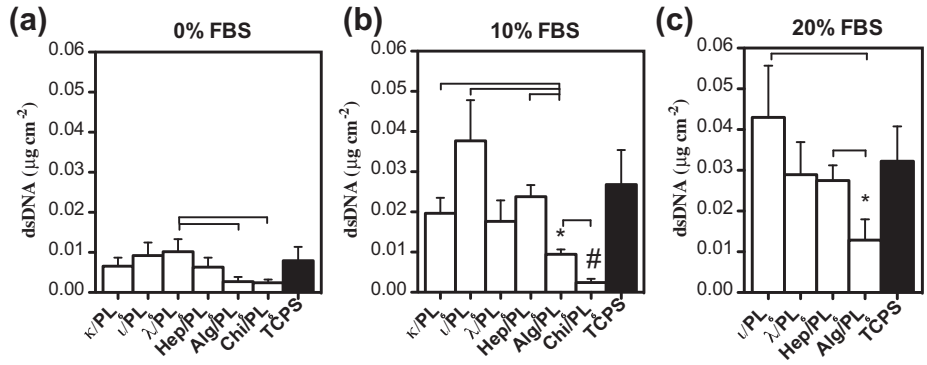

Fig. 2. HUVECs adhesion after 20 h in culture in absence of ECGS and: (a) 0% FBS, (b) 10% FBS, (c) 20% FBS. All significances are indicated with: * (different to TCPS), # (different to all) and bars (pair is different), ($p < 0.05$, $n = 6$; mean ± sem).

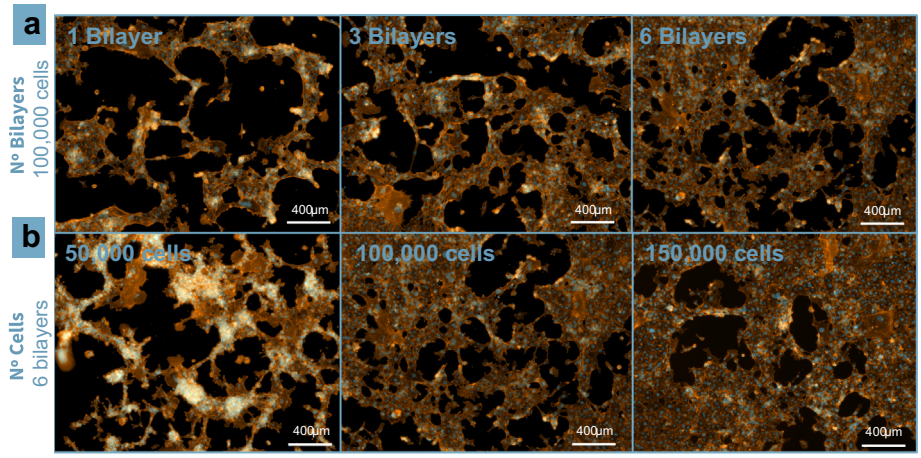

Fig. 3. EC morphology onto several λ/PL multilayers, after 20 h of culture, in presence of 10% FBS and absence of ECGS and Hep. (a) Morphology on multilayers with different number of bilayers: λ/PL1, λ/PL3 and λ/PL6. (b) Effect of seeding density on the morphology of HUVECs on λ/PL6 multilayers. (nuclei: blue, actin fibers: orange). (For interpretation of the references to colour in this figure legend, the reader is referred to the web version of this article.)

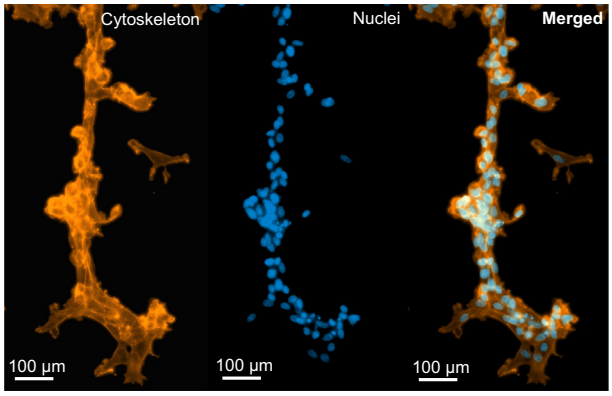

Fig. 4. Representative image of HUVECS assembled into a tube-like structure after 20 h in culture (nuclei: blue, actin fibers: orange). (For interpretation of the references to colour in this figure legend, the reader is referred to the web version of this article.)

The number of bilayers forming the nanocoatings could also affect the density of instructive proteins presented to the cells. Thereby, the cell seeding density of HUVECs and the number of bilayers of the λ/PL pair were also varied. Respectively, 50,000, 100,000 and 150,000 cells/cm^2 were seeded on λ/PL$_6$, and 100,000 cells/cm^2 seeded on nanocoatings prepared with 1, 3 and 6 bilayers (λ/PL$_1$, λ/PL$_3$ and λ/PL$_6$) – Fig. 3. Total tube-length, number of meshes, number of nodes and master junctions formed were quantified on fluorescence images (5×) using Angiogenesis Analyzer for Image J – Fig. 5. A single bilayer of λ/PL was sufficient to promote the formation of a network with 100,000 cells, which total tube length could be increased with increasing number of layers. With 6 bilayers, a lower cell density has shown to be more adequate in obtaining a better network formation than with fewer layers. This indicates that cell adhesion and TLS are dependent on the number of bilayers and increasing the number of layers allows a decrease of the required cell density.

Besides the total tube length, the number of nodes and meshes were also influenced by the number of layers. It was observed a tendency of increase all the features with the increasing of the number of layers. In general, Hep/PL$_6$ (100,000 cells) and λ/PL$_6$ (50,000 cells) have shown similar results, though a higher number of total nodes was observed on λCar.

Cell Profiler was used to analyze cell form factor (i.e., roundness), eccentricity (i.e., elongation), major axis (i.e., cell length) and minor axis (i.e., cell width) – Fig. S3. This analysis revealed that under the tested conditions, the EC morphology was significantly changed when seeded on the multilayers in comparison to TCPS. While on TCPS cells show the normal cobblestone-like morphology, they become rounder on the instructive multilayers (form factor closer to 1). However, on the multilayers that successfully induced TLS, the cells elongation factor was similar to TCPS. Both width and length decreased on the multilayers, thus not altering significantly the elongation relatively to TCPS.

Please cite this article in press as: S.M. Oliveira et al., Platelet lysate-based pro-angiogenic nanocoatings, Acta Biomater. (2015), http://dx.doi.org/10.1016/j.actbio.2015.12.028

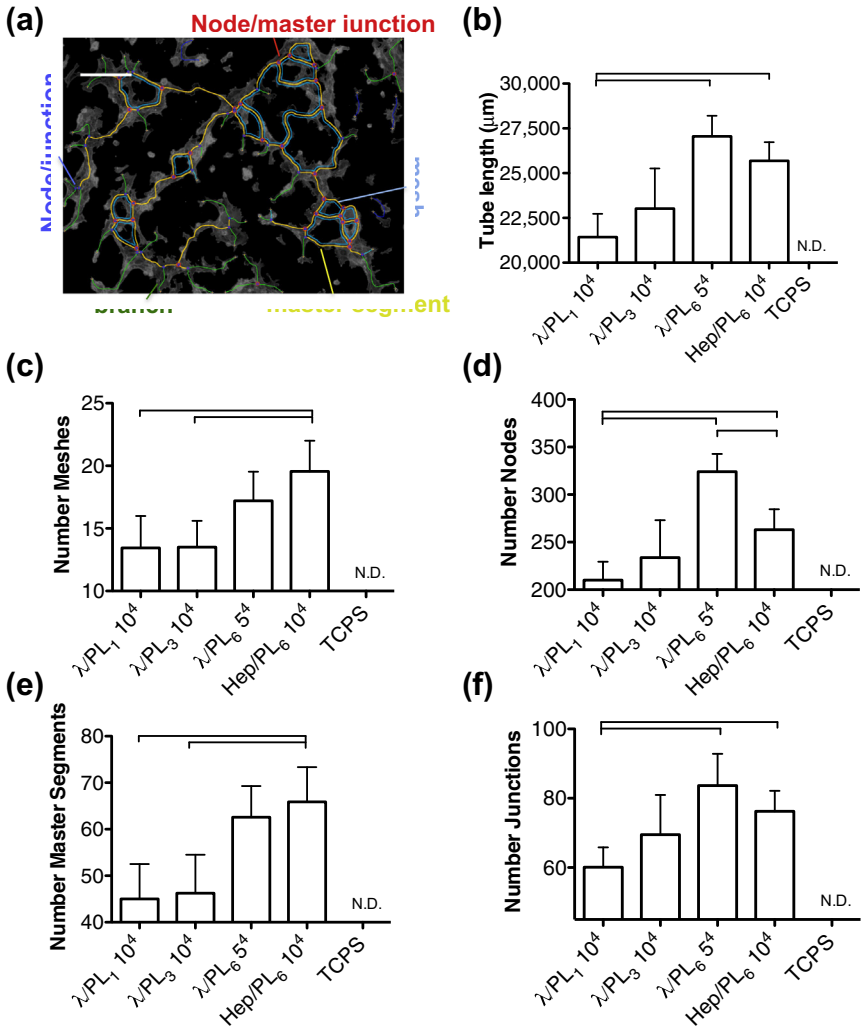

Fig. 5. (a) Angiogenic parameters quantified with Angiogenesis Analyzer on cytoskeleton-stained images; (b) total tube length; (c) number of meshes; (d) number of nodes; (e) number of master segments; (f) number of junctions. All pairs of samples were compared and significances are indicated with bars ($p < 0.05$, $n = 6$, mean ± sem). 5^4 = 50,000 cells/cm^2; 10^4 = 100,000 cells/cm^2; 15^4 = 150,000 cells/cm^2.

Frequently, on hydrogel-like basement membranes, cells tend to be more elongated after 20–24 h of incubation. [38] Herein, the surface properties (non-gel), the time of incubation and the cell number may have caused the reduction of the size and the lack of cytoskeleton elongation.

3.3. Endothelial cells proliferation

In order to assess cell proliferation capability, the medium was replaced with fresh medium with or without ECGS-Hep and cells were incubated for more 3 days – Fig. 6a and b. Morphology was observed after 4 days in culture – Fig. 6c. Even though the initial media was changed, removing possible released GFs, HUVECs kept some cell alignment after 4 days in culture on λPL$_6$ (50,000 cells/cm^2). On the other hand, in presence of ECGS cells have lost the TLS and reached confluence.

Independently of the surface, in absence of growth supplement, cells were unable to proliferate. In particular, Hep/PL$_6$ has not supported cell viability, and cell number was slightly reduced ($p < 0.05$) which suggests a lower pro-survival stimulation.

Medium supplementation with ECGS allowed a minimal proliferation of the ECs, being this effect more pronounced on TCPS ($p < 0.05$). Among the multilayers, ι/PL$_6$ showed the highest HUVECs proliferation. This improvement might be related with the higher capability of ιCar to incorporate FGFb, which growth factor is reported to be able of stimulating EC proliferation [39]. Nonetheless, the overall behavior suggested that these multilayers do not promote ECs proliferation, and TLS formation in some cases. This corroborates the reported tendency of matrices that lead to extensive tubule formation (e.g., collagen IV, V and Matrigel) of allowing only a minimal EC proliferation [6,40]. This proliferation inhibition effect could be promoted by specific GFs that are simultaneously capable of eliciting the formation of TLS and inhibit EC proliferation. For instance, transforming growth factor beta 1 (TGF-β1) induces angiogenesis through VEGF A-mediated apoptosis [41]. TGF-β1 is one of the multiple GF that can be found in PL. The simultaneous presence of TGF-β1 and other GFs, rather than only promoting angiogenesis or mitogenesis (e.g., by FGFb and VEGF A, PDGF), could both elicit angiogenesis and impair proliferation or cell apoptosis.

3.4. Angiogenic-gene expression

During the angiogenesis stages (activation, proliferation, migration and stabilization) the gene expression of the ECs is regulated by several pro and anti-angiogenic factors. GFs such as VEGF A

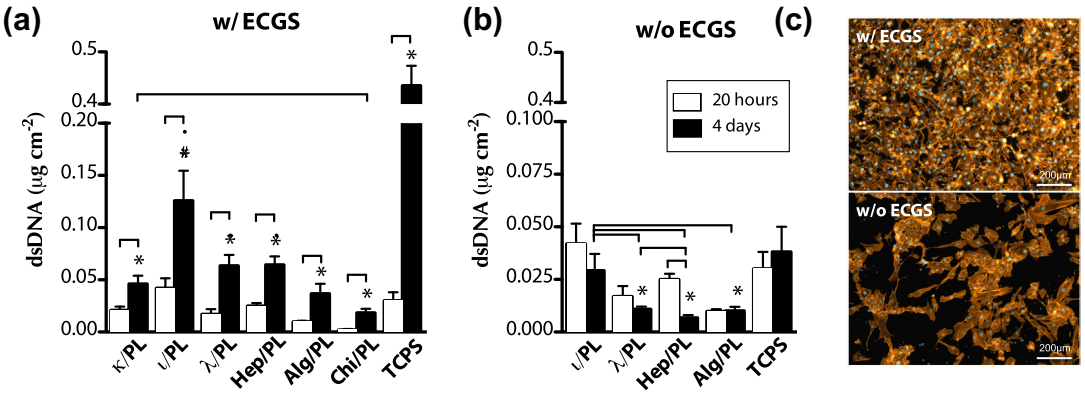

Fig. 6. Proliferation of HUVECs cultured with 10% FBS and in absence (a), or presence of ECGS-hep (b), after adhesion for 20 h (in absence of ECGS-hep and with 10% FBS). All significances are indicate with: * (different to TCPS), # (different to all, after 4 days), (different to Chi/PL and Alg/PL) and bars (pair is different), ($p < 0.05$, $n = 6$; mean ± sem). (c) HUVECs (λ/PL_6 50,000 cells/cm^2) morphology after 4 days in culture showing some remaining TLS when cultured in absence of ECGS-hep (10%FBS), while in presence of ECGS-hep (10%FBS) cells had disassembled, proliferated and reached confluence.

and FGFb activate ECs and promote their proliferation. Integrin such as α5, αν, β3 play important roles during EC migration while angiopoietin-1, PDGF and TGF-β regulate maturation and vessels stabilization [8,42,43]. Herein, gene expression of VEGFA, FGFb, integrins (α5, αν and β3) and angiopoietin-1 were quantified after 20 h of culture – Fig. 7.

In accordance with the literature, the angiogenic-gene expression alterations during TLS formation are expected to be of small magnitude (<2-fold) or even negative, as related to TCPS [42,44]. Indeed, for the majority of conditions, gene expression was similar or significantly lower than TCPS with the exception of the expression of VEGFA and angiopoietin-1. Regarding the expression of integrins, λ/PL_6 (50,000 cells), λ/PL_3 (100,000 cells), ι/PL_6 (100,000 cells) and Hep/PL_6 (100,000 cells) have, in general, shown lower or similar expression to TCPS ($p < 0.05$). Exogenous FGFb is known to be able to promote angiogenesis, both *in vivo* and *in vitro*, by up-regulating the expression of VEGFA and the endogenous VEGFA in ECs [45]. However, the expression of FGFb was decreased on ι/PL_6 (100,000 cells), λ/PL_3 (100,000 cells), λ/PL_6 (50,000 cells), λ/PL_6 (100,000 cells), with exception of Hep/PL_6.

Both VEGFA and angiopoietin-1 are strong pro-angiogenic factors with distinct functions and bidirectional dependent: one up-regulates the other. While VEGFA causes vascular permeability, angiopoietin-1 stabilizes the blood vessels and avoids plasma leakage induced by VEGFA [46,47]. Although being frequently related with different angiogenesis stages, the simultaneously stimulation of ECs with VEGFA and angiopoietin-1 has previously shown a synergistic improvement of angiogenesis [48].

Recently, it has been reported that PRP contains high amounts of angiopoietin-1 (~300fold more than VEGFA) [16]. The same study has shown that angiopoietin-1 and its respective cell receptor (Tie2) are crucial in promoting angiogenesis when using a preparation of 250-fold diluted PRP.

Both the expression of VEGF A and angiopoietin-1 were simultaneously increased with exception of TCPS, Alg/PL_6 and ι/PL_6. Angiopoietin-1 was increased even on the multilayers not promoting TLS which suggests that surface VEGFA or FGFb (which primarily up-regulates VEGFA [45]) might have up-regulated angiopoietin-1 [49]. If a significant amount of angiopoietin-1 had been incorporated in the coatings, this could up-regulate VEGFA

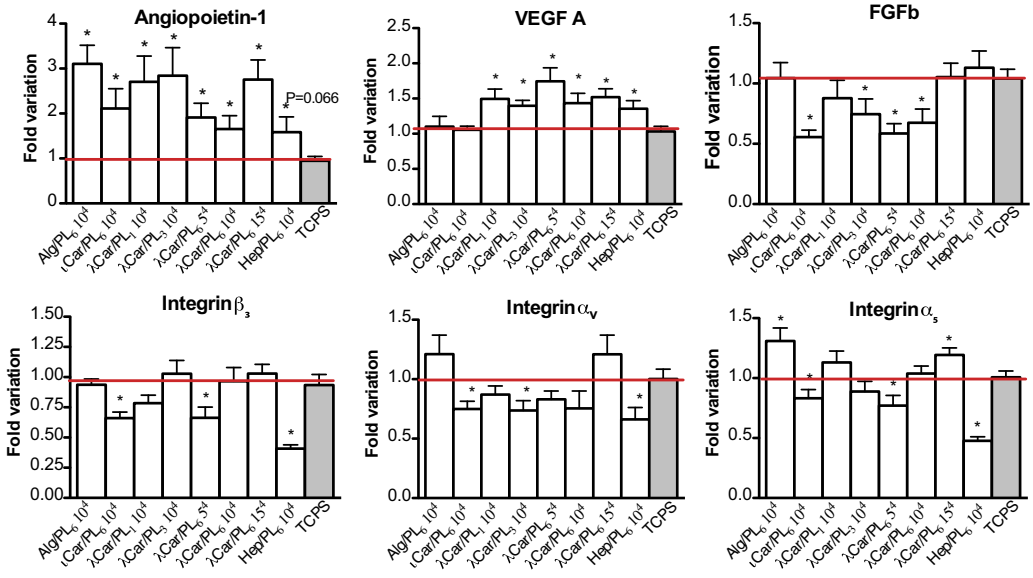

Fig. 7. Gene expression-fold variation of Angiopoietin-1, VEGF A, FGFb and integrins α_v, α_5, β_3 relatively to TCPS. The expression of theses genes was normalized against the housekeeping β-actin gene or GAPHD (in case of VEGFA) and calculated by the Livak method ($2^{-\Delta\Delta Ct}$). Samples were compared with the control (TPCS) and differences are identified with * ($p < 0.05$, $n = 8$, mean ± sem).

Please cite this article in press as: S.M. Oliveira et al., Platelet lysate-based pro-angiogenic nanocoatings, Acta Biomater. (2015), http://dx.doi.org/10.1016/j.actbio.2015.12.028

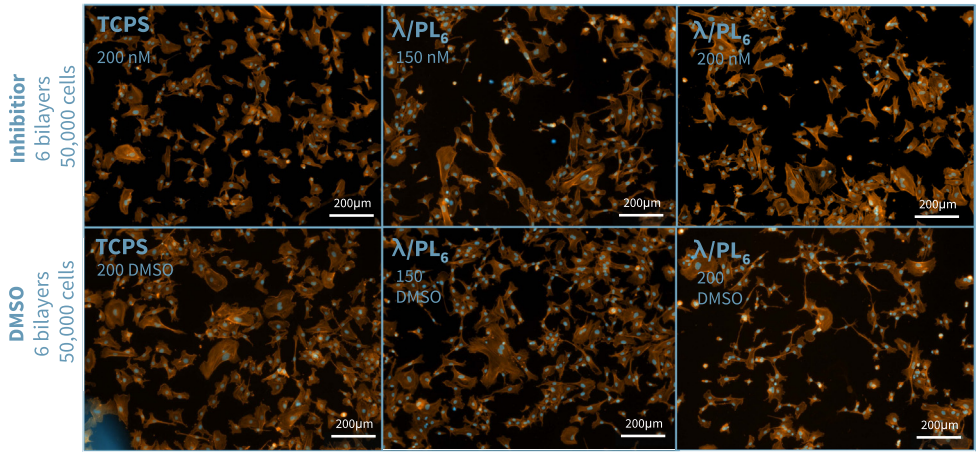

Fig. 8. Cell morphology of HUVECs seeded on λ/PL_6 and TPCs in presence of VEGF/FGF receptor kinase inhibitor (or DMSO) inhibiting the formation of TLS. (cytoskeleton: orange; nuclei: blue). (For interpretation of the references to colour in this figure legend, the reader is referred to the web version of this article.)

expression and VEGFA endogenous content, and consequently, indirectly stimulate the formation of TLS [48,50,51].

3.5. Blockage of FGF/VEGF tyrosine kinase receptor

HUVECs were cultured in the presence of a FGF/VEGF tyrosine kinase receptor inhibitor to understand whether the morphogenic changes were driven by those pro-angiogenic GFs. This compound could block the interaction of FGF and VEGF from the nanocoating, or the soluble form, with their respective cell receptors (e.g., FGFR2 and VEGFR2). A condition that was shown to induce TLS was selected: 50,000 cells/cm^2 onto λ/PL_6. Cells were seeded with a supplier's recommended range of concentrations of inhibitor dissolved with DMSO (150 nM and 200 nM, containing 0.0075% v/v and 0.01% v/v DMSO, respectively) or only with DMSO (0.0075% v/v and 0.01% v/v of DMSO – named DMSO 150 and DMSO 200) during 20 h. The use of DMSO as a solvent has diminished the observed cellular density and made cells more elongated – Fig. 8. However, the ability of HUVECS to be more cohesive and to align was further reduced with the presence of the inhibitor and with its increased concentration. No TLS were observed on the surfaces. Cell Profiler analysis has not revealed significant cell shape differences between λ/PL_6 (50,000 cells) with inhibitor and only with DMSO, both for 150 nM and for 200 nM – Fig. S3. DMSO is reported as being able to decrease cell adhesion even at low concentrations (1.55% v/v) [52]. Concentrations higher than 1% v/v have also been reported to impair the formation of TLS on Matrigel [53]. Thereby, one cannot exclude the inhibition of TLS and changes in cell morphology to be in part caused by DMSO. Nonetheless, there are indications that at least at some extent, FGF/VEGF has mediated the formation of TLS.

The PL coatings assembled with the more sulfated polysaccharides were able to induce a pro-angiogenic profile in HUVECs. This strategy may be a cost-effective way to introduce pro-angiogenic interfaces on surfaces or 3D scaffolds.

4. Conclusions

There is still a current need to develop cost effective cell-interfaces able to promote angiogenesis and the formation of stable vasculature.

PL is a source of several pro-angiogenic and other proteins involved in the angiogenesis from the earliest to the maturation phases. Herein, PL was incorporated in layer-by-layer assembled nanocoatings with varied polysaccharides and number of layers. The nanocoatings prepared with the more sulfated polysaccharides elicited the formation of tube-like structures in ECs within 20 h of incubation. These morphogenic changes were accompanied by differences in gene expressions, mainly higher VEGFA and higher angiopoietin-1. Future work must be performed in order to clarify the rule of PL as well as the *in vivo* behavior of the developed structures.

Layer-by-Layer assembling including PL might be a simple methodology to introduce and tune cost-effective pro-angiogenic interfaces in 2D/3D biomaterials.

Acknowledgments

The research leading to these results has received funding from European Union's Seventh Framework Program (FP7/2007-2013) under grant agreement nª REGPOT-CT2012-316331 – POLARIS and FP7-KBBE-2010-4-266033 – SPECIAL. This work was also supported by the European Research Council grant agreement ERC-2012-ADG-20120216-321266 for the project ComplexiTE. Portuguese Foundation for Science and Technology is gratefully acknowledged for fellowship of Sara M. Oliveira (SFRH/BD/70107/2010). The researcher contract of R.P. Pirraco through RL3-TECT-NORTE-01-0124-FEDER-000020, co-financed by North Portugal Regional Operational Program (ON.2-O Novo Norte), under the National Strategic Reference Framework, through the European Regional Development Fund is also acknowledged.

Appendix A. Supplementary data

Supplementary data associated with this article can be found, in the online version, at http://dx.doi.org/10.1016/j.actbio.2015.12.028.

References

[1] F.A. Auger, L. Gibot, D. Lacroix, The pivotal role of vascularization in tissue engineering, Annu. Rev. Biomed. Eng. 15 (2013) 177–200.
[2] E.C. Novosel, C. Kleinhans, P.J. Kluger, Vascularization is the key challenge in tissue engineering, Adv. Drug Delivery Rev. 63 (2011) 300–311.
[3] M.I. Santos, R.L. Reis, Vascularization in bone tissue engineering: physiology, current strategies, major hurdles and future challenges, Macromol. Biosci. 10 (2010) 12–27.
[4] Y.J. Blinder, D.J. Mooney, S. Levenberg, Engineering approaches for inducing blood vessel formation, Curr. Opin. Chem. Eng. 3 (2014) 56–61.
[5] L.E. Bertassoni, M. Cecconi, V. Manoharan, M. Nikkhah, J. Hjortnaes, A.L. Cristino, G. Barabaschi, D. Demarchi, M.R. Dokmeci, Y. Yang, A. Khademhosseini, Hydrogel bioprinted microchannel networks for vascularization of tissue engineering constructs, Lab Chip 14 (2014) 2202–2211.

[6] C.A. Staton, M.W. Reed, N.J. Brown, A critical analysis of current in vitro and in vivo angiogenesis assays, Int. J. Exp. Pathol. 90 (2009) 195–221.
[7] M.W. Irvin, A. Zijlstra, J.P. Wikswo, A. Pozzi, Techniques and assays for the study of angiogenesis, Exp. Biol. Med. (Maywood) 239 (2014) 1476–1488.
[8] X.M. van Wijk, T.H. van Kuppevelt, Heparan sulfate in angiogenesis: a target for therapy, Angiogenesis 17 (2014) 443–462.
[9] M. Matsui, Y. Tabata, Enhanced angiogenesis by multiple release of platelet-rich plasma contents and basic fibroblast growth factor from gelatin hydrogels, Acta Biomater. 8 (2012) 1792–1801.
[10] G. Sufen, Y. Xianghong, C. Yongxia, P. Qian, bFGF and PDGF-BB have a synergistic effect on the proliferation, migration and VEGF release of endothelial progenitor cells, Cell Biol. Int. 35 (2011) 545–551.
[11] G. Sun, Y.I. Shen, S. Kusuma, K. Fox-Talbot, C.J. Steenbergen, S. Gerecht, Functional neovascularization of biodegradable dextran hydrogels with multiple angiogenic growth factors, Biomaterials 32 (2011) 95–106.
[12] Q. Sun, E.A. Silva, A. Wang, J.C. Fritton, D.J. Mooney, M.B. Schaffler, P.M. Grossman, S. Rajagopalan, Sustained release of multiple growth factors from injectable polymeric system as a novel therapeutic approach towards angiogenesis, Pharm. Res. 27 (2010) 264–271.
[13] K. Stellos, S. Kopf, A. Paul, J.U. Marquardt, M. Gawaz, J. Huard, H.F. Langer, Platelets in Regeneration. Seminars in Thrombosis and Hemostasis, Thieme Medical Publishers, 2010. p. 175–84.
[14] S.C. Bir, J. Esaki, A. Marui, K. Yamahara, H. Tsubota, T. Ikeda, R. Sakata, Angiogenic properties of sustained release platelet-rich plasma: characterization in-vitro and in the ischemic hind limb of the mouse, J. Vasc. Surg. 50 (2009) 870–879. e2.
[15] N. Kakudo, N. Morimoto, S. Kushida, T. Ogawa, K. Kusumoto, Platelet-rich plasma releasate promotes angiogenesis in vitro and in vivo, Med. Mol. Morphol. 47 (2014) 83–89.
[16] T. Mammoto, A. Jiang, E. Jiang, A. Mammoto, Platelet rich plasma extract promotes angiogenesis through the angiopoietin1-Tie2 pathway, Microvasc. Res. 89 (2013) 15–24.
[17] B. Zhou, J. Ren, C. Ding, Y. Wu, D. Hu, G. Gu, J. Li, Rapidly in situ forming platelet-rich plasma gel enhances angiogenic responses and augments early wound healing after open abdomen, Gastroenterol. Res. Pract. 2013 (2013). 926764.
[18] Y. Man, P. Wang, Y. Guo, L. Xiang, Y. Yang, Y. Qu, P. Gong, L. Deng, Angiogenic and osteogenic potential of platelet-rich plasma and adipose-derived stem cell laden alginate microspheres, Biomaterials 33 (2012) 8802–8811.
[19] F. Findikcioglu, K. Findikcioglu, R. Yavuzer, N. Lortlar, K. Atabay, Effect of preoperative subcutaneous platelet-rich plasma and fibrin glue application on skin flap survival, Aesthetic Plast. Surg. 36 (2012) 1246–1253.
[20] J. Leotot, L. Coquelin, G. Bodivit, P. Bierling, P. Hernigou, H. Rouard, N. Chevallier, Platelet lysate coating on scaffolds directly and indirectly enhances cell migration, improving bone and blood vessel formation, Acta Biomater. 9 (2013) 6630–6640.
[21] E. Polykandriotis, A. Arkudas, R.E. Horch, U. Kneser, G. Mitchell, To matrigel or not to matrigel, Am. J. Pathol. 172 (2008) 1441–1442.
[22] J. Borges, J.F. Mano, Molecular interactions driving the layer-by-layer assembly of multilayers, Chem. Rev. 114 (2014) 8883–8942.
[23] R.R. Costa, J.F. Mano, Polyelectrolyte multilayered assemblies in biomedical technologies, Chem. Soc. Rev. 43 (2014) 3453–3479.
[24] S.M. Oliveira, T.H. Silva, R.L. Reis, J.F. Mano, Nanocoatings containing sulfated polysaccharides prepared by layer-by-layer assembly as models to study cell-material interactions, J. Mater. Chem. B 1 (2013) 4406–4418.
[25] K. Gaengel, C. Betsholtz, Endocytosis regulates VEGF signalling during angiogenesis, Nat. Cell Biol. 15 (2013) 233–235.
[26] S.M. Oliveira, V.E. Santo, M.E. Gomes, R.L. Reis, J.F. Mano, Layer-by-layer assembled cell instructive nanocoatings containing platelet lysate, Biomaterials 48 (2015) 56–65.
[27] J. Kreuger, D. Spillmann, J.P. Li, U. Lindahl, Interactions between heparan sulfate and proteins: the concept of specificity, J. Cell Biol. 174 (2006) 323–327.
[28] G.S. Schultz, A. Wysocki, Interactions between extracellular matrix and growth factors in wound healing, Wound Repair Regen. 17 (2009) 153–162.
[29] S.K. Nigam, K.T. Bush, Growth factor-heparan sulfate "switches" regulating stages of branching morphogenesis, Pediatr. Nephrol. 29 (2014) 727–735.
[30] T.H. Nguyen, S.H. Kim, C.G. Decker, D.Y. Wong, J.A. Loo, H.D. Maynard, A heparin-mimicking polymer conjugate stabilizes basic fibroblast growth factor, Nat. Chem. 5 (2013) 221–227.
[31] T.N. Vo, F.K. Kasper, A.G. Mikos, Strategies for controlled delivery of growth factors and cells for bone regeneration, Adv. Drug Delivery Rev. 64 (2012) 1292–1309.
[32] T.H. Silva, A. Alves, B.M. Ferreira, J.M. Oliveira, L.L. Reys, R.J.F. Ferreira, R.A. Sousa, S.S. Silva, J.F. Mano, R.L. Reis, Materials of marine origin: a review on polymers and ceramics of biomedical interest, Int. Mater. Rev. 57 (2012) 276–307.
[33] K. Senni, J. Pereira, F. Gueniche, C. Delbarre-Ladrat, C. Sinquin, J. Ratiskol, G. Godeau, A.M. Fischer, D. Helley, S. Colliec-Jouault, Marine polysaccharides: a source of bioactive molecules for cell therapy and tissue engineering, Mar. Drugs 9 (2011) 1664–1681.
[34] J.F. Mano, G.A. Silva, H.S. Azevedo, P.B. Malafaya, R.A. Sousa, S.S. Silva, L.F. Boesel, J.M. Oliveira, T.C. Santos, A.P. Marques, N.M. Neves, R.L. Reis, Natural origin biodegradable systems in tissue engineering and regenerative medicine: present status and some moving trends, J. R. Soc. Interface 4 (2007) 999–1030.
[35] S.M. Oliveira, R.L. Reis, J.F. Mano, Assembling human platelet lysate into multiscale 3D scaffolds for bone tissue engineering, ACS Biomater. Sci. Eng. 1 (2015) 2–6.
[36] J.F. Mano, Designing biomaterials for tissue engineering based on the deconstruction of the native cellular environment, Mater. Lett. 141 (2015) 198–202.
[37] M.G. Lampugnani, F. Orsenigo, M.C. Gagliani, C. Tacchetti, E. Dejana, Vascular endothelial cadherin controls VEGFR-2 internalization and signaling from intracellular compartments, J. Cell Biol. 174 (2006) 593–604.
[38] P.J. Stahl, T.R. Chan, Y.I. Shen, G. Sun, S. Gerecht, S. Yu, Capillary network-like organization of endothelial cells in PEGDA scaffolds encoded with angiogenic signals via triple helical hybridization, Adv. Funct. Mater. 24 (2014) 3213–3225.
[39] A. Sahni, C.W. Francis, Stimulation of endothelial cell proliferation by FGF-2 in the presence of fibrinogen requires αvβ32004, Blood 104 (2004) 3635–3641.
[40] J.A. Madri, S.K. Williams, Capillary endothelial cell cultures: phenotypic modulation by matrix components, J. Cell Biol. 97 (1983) 153–165.
[41] G. Ferrari, B.D. Cook, V. Terushkin, G. Pintucci, P. Mignatti, Transforming growth factor-beta 1 (TGF-β1) induces angiogenesis through vascular endothelial growth factor (VEGF)-mediated apoptosis, J. Cell. Physiol. 219 (2009) 449–458.
[42] R. Mammadov, B. Mammadov, S. Toksoz, B. Aydin, R. Yagci, A.B. Tekinay, M.O. Guler, Heparin mimetic peptide nanofibers promote angiogenesis, Biomacromolecules 12 (2011) 3508–3519.
[43] K.P. Claffey, Molecular profiling of angiogenic markers: a step towards interpretive analysis of a complex biological function, Am. J. Pathol. 161 (2002) 7–11.
[44] A.D. Grove, V.V. Prabhu, B.L. Young, F.C. Lee, V. Kulpa, P.J. Munson, E.C. Kohn, Both protein activation and gene expression are involved in early vascular tube formation in vitro, Clin. Cancer Res. 8 (2002) 3019–3026.
[45] G. Seghezzi, S. Patel, C.J. Ren, A. Gualandris, G. Pintucci, E.S. Robbins, R.L. Shapiro, A.C. Galloway, D.B. Rifkin, P. Mignatti, Fibroblast growth factor-2 (FGF-2) induces vascular endothelial growth factor (VEGF) expression in the endothelial cells of forming capillaries: an autocrine mechanism contributing to angiogenesis, J. Cell Biol. 141 (1998) 1659–1673.
[46] J. Gavard, V. Patel, J.S. Gutkind, Angiopoietin-1 prevents VEGF-induced endothelial permeability by sequestering Src through mDia, Dev. Cell 14 (2008) 25–36.
[47] S.P. Ngok, R. Geyer, M. Liu, A. Kourtidis, S. Agrawal, C. Wu, H.R. Seerapu, L.J. Lewis-Tuffin, K.L. Moodie, D. Huveldt, R. Marx, J.M. Baraban, P. Storz, A. Horowitz, P.Z. Anastasiadis, VEGF and Angiopoietin-1 exert opposing effects on cell junctions by regulating the Rho GEF Syx, J. Cell Biol. 199 (2012) 1103–1115.
[48] T.I. Koblizek, C. Weiss, G.D. Yancopoulos, U. Deutsch, W. Risau, Angiopoietin-1 induces sprouting angiogenesis in vitro, Curr. Biol. 8 (1998) 529–532.
[49] M. Hangai, T. Murata, N. Miyawaki, C. Spee, J.I. Lim, S. He, D.R. Hinton, S.J. Ryan, Angiopoietin-1 upregulation by vascular endothelial growth factor in human retinal pigment epithelial cells, Invest. Ophthalmol. Vis. Sci. 42 (2001) 1617–1625.
[50] W.H. Zhu, A. MacIntyre, R.F. Nicosia, Regulation of angiogenesis by vascular endothelial growth factor and angiopoietin-1 in the rat aorta model: distinct temporal patterns of intracellular signaling correlate with induction of angiogenic sprouting, Am. J. Pathol. 161 (2002) 823–830.
[51] S. Kanda, H. Kanetake, Y. Miyata, Role of Src in angiopoietin 1-induced capillary morphogenesis of endothelial cells: Effect of chronic hypoxia on Src inhibition by PP2, Cell. Signal. 19 (2007) 472–480.
[52] N. Eter, M. Spitznas, DMSO mimics inhibitory effect of thalidomide on choriocapillary endothelial cell proliferation in culture, Br. J. Ophthalmol. 86 (2002) 1303–1305.
[53] K. Koizumi, Y. Tsutsumi, Y. Yoshioka, M. Watanabe, T. Okamoto, Y. Mukai, S. Nakagawa, T. Mayumi, Anti-angiogenic effects of dimethyl sulfoxide on endothelial cells, Biol. Pharm. Bull. 26 (2003) 1295–1298.

Please cite this article in press as: S.M. Oliveira et al., Platelet lysate-based pro-angiogenic nanocoatings, Acta Biomater. (2015), http://dx.doi.org/10.1016/j.actbio.2015.12.028